Hindawi
Advances in Civil Engineering
Volume 2019, Article ID 4347302, 19 pages
https://doi.org/10.1155/2019/4347302

*Research Article*

# Application of Constant Resistance and Large Deformation Anchor Cable in Soft Rock Highway Tunnel

**Xiaoming Sun**[1], **Bo Zhang**[1,2], **Li Gan**[1,2], **Zhigang Tao**[1] and **Chengwei Zhao**[1,2]

[1]*State Key Laboratory for Geomechanics & Deep Underground Engineering, Beijing 100083, China*
[2]*School of Mechanics and Civil Engineering, China University of Mining & Technology, Beijing 100083, China*

Correspondence should be addressed to Xiaoming Sun; 108830@cumtb.edu.cn and Zhigang Tao; taozhigang@263.net

Received 22 April 2019; Revised 24 June 2019; Accepted 14 July 2019; Published 31 July 2019

Academic Editor: Flora Faleschini



Muzhailing Highway Extra-long Tunnel in Lanzhou, Gansu Province, China, belongs to the soft rock tunnel in the extremely high geostress area. During the construction process, large deformation of the soft rock occurred frequently. Taking the no. 2 inclined shaft of Muzhailing tunnel as the research object, an NPR (negative Poisson's ratio) constant resistance and large deformation anchor cable support system based on high prestress force, constant resistance, and releasing surrounding rock pressure was proposed. The characteristics of the surrounding rock under the steel arch support and NPR anchor cable support were compared and analyzed by using 3DEC software. A series of field tests were conducted in the no. 2 inclined shaft, and the rock strength, displacement of the surrounding rock, deep displacement of the surrounding rock, internal force of steel arch, and axial force of anchor cable were measured to study the application effect of the NPR anchor cable support system in tunnel engineering. Moreover, the 3DEC numerical simulation results were compared with the field test results. The research results show that the application of NPR constant resistance and large deformation anchor cable support system in tunnel engineering has achieved good results, and it plays a significant role in controlling the large deformation of the tunnel surrounding rock.

## 1. Introduction

With the rapid development of tunnel engineering in the modern world, the construction of railway and highway tunnels in China has developed by leaps and bounds in recent years. Among them, soft surrounding rock tunnels account for a large proportion and are prone to large deformation of the soft rock in the construction process. Muzhailing railway tunnel and Muzhailing highway tunnel are typical, and the Muzhailing tunnel of the Lanzhou-Chongqing railway is one of the most high-risk tunnels in China. The total length of the tunnel is 19.1 km. The cross-sectional area is about 70 $m^2$. The construction lasted eight years, but deformation, cracking, and dislocation still occurred three years after the completion of some parts. Therefore, the construction of Muzhailing Highway Extra-long Tunnel is a difficult problem in tunnel engineering at present.

Researchers have done a lot of research on the deformation and support methods of the tunnel surrounding rock. Hoek et al. [1] studied rock strength and rock mass strength, as well as the deformation characteristics of tunnels at different depths. They considered that rock mass strength and ground stress were the key factors affecting the stability of the tunnel surrounding rock. Meguid and Rowe [2] used a three-dimensional numerical simulation method to study the deformation law and stress distribution law of the tunnel surrounding rock under different stresses. Brox and Hagedorn [3] studied the deformation characteristics of Anatolian Expressway tunnel crossing faults in Turkey. They considered that tectonic stress, weak surrounding rock, and stress concentration after excavation were the main reasons for tunnel deformation. Lai et al. [4] analyzed a tunnel in the Qinling-Bashan strong tectonic stress area, which was mainly composed of soft rocks such as phyllite-slate. By studying the deformation characteristics of the tunnel

support before and after, a combined support method of advance pipe umbrella + presupport advance pipe + prestrengthening cartridge bolt + foot-lock bolt was proposed, and good results were obtained. Guojun et al. [5] studied the performance of foamed concrete and put forward a supporting strategy for pouring foamed concrete between primary support and secondary lining. According to the numerical simulation analysis, they found that the support scheme can effectively control the stress state of the primary lining and the plastic zone of the second lining. Merlini et al. [6] studied the deformation mechanism of the soft rock in the Ceneri Base extra-long tunnel and proposed a combined support scheme of deformable bracket + anchor net shotcrete + shotcrete reinforced with fibers + steel arch, which could effectively control the tunnel surrounding rock subsidence. Zhang et al. [7] proposed that the key problem of NATM construction in the soft rock tunnel was the stability of the surrounding rock of the working face. A mechanical model of the surrounding rock structure based on the limit equilibrium method was established. The relationship between surrounding rock stress, tunnel depth, and bolt support strength was analyzed. It was found that tunnel bolt can effectively improve the shear strength of the surrounding rock.

The traditional tunnel support measures cannot adapt to the special thin-bedded slate surrounding rock of the Muzhailing tunnel, and a new support system needs to study urgently. This paper introduced the application of NPR constant resistance and large deformation anchor cable support system in tunnels. The steel arch support and NPR anchor support were compared and analyzed using the 3DEC numerical simulation software. The results of the field monitoring test show that the NPR constant resistance large deformation anchor cable has achieved good results in controlling the surrounding rock deformation.

## 2. Project Overview

As shown in Figure 1, Muzhailing tunnel is located in Lanzhou, Gansu Province, China. It is a key control project of the Lanzhou-Haikou national expressway. The length of the tunnel is 15.226 km. It is the longest tunnel on the whole line with a maximum depth of 629.1 m. The excavation area is larger than 133.8 $m^2$, and some parts of the tunnel are deeper than 500 m over 60% of the total length. This paper relies on the no. 2 inclined shaft of Muzhailing tunnel to explore the supporting measures of the soft rock tunnel. The inclined shaft is 1813.43 m in length and 591 m in maximum depth.

*2.1. Geological Survey.* According to geological exploration, the geostress of the surrounding rock of the no. 2 inclined shaft was 15.7 MPa, the maximum horizontal principal stress was 24.95 MPa, and the rock strength was less than 30 MPa. According to the Standard for Engineering Classification of Rock Mass (GB/50218-94), the $R_c/\sigma_{max}$ value is less than 4 ($R_c$ is uniaxial saturated compressive strength of the rock and $\sigma_{max}$ is the stress of the tunnel), so the tunnel belongs to the extremely high geostress tunnel. The rock stratum is relatively fragmented, and the possibility of large deformation of the tunnel surrounding rock is high. The direction of maximum horizontal principal stress measured by the hydraulic fracturing method was near NE39.6° and NE34.1°, which indicated that the direction of maximum principal stress in the exploration area was NE. The measured results are close to the regional tectonic stress field inferred from the geological structure. Considering the geostress, the angle between the maximum horizontal principal stress direction and the axis direction of the Muzhailing tunnel is 0°~30°. The angle between the maximum horizontal principal stress direction and the axis direction of the no. 2 inclined shaft is 60°~90°. Therefore, these two factors are not conducive to the stability of the tunnel. The surrounding rock of the tunnel is mainly composed of carbonaceous slate with a grey-black and thin-layer structure. The dip angle of the stratum is between 30° and 85°, and the slate thickness is between 5 cm and 30 cm. There are sandstones, limestones, shale interbeds, and few quartz in the strata. Moreover, the carbonaceous slate has the characteristics of expansibility, disintegration, rheology, and sensitivity to engineering disturbance. Figure 2 shows the exposed tunnel surrounding rock.

*2.2. Form of Original Tunnel Support.* The original supporting design principle of the no. 2 inclined shaft was NATM, which adopted three-bench excavation form, as shown in Figure 3. The tunnel is about 13 m wide and 10.7 m high, and its excavation area is about 113 $m^2$. It belongs to the super large cross-section tunnel, as shown in Figure 4. Because the surrounding rock was affected by high geostress and complex geological conditions, the problem of large deformation of the soft rock in tunnel construction was very serious. The deformation of the tunnel surrounding rock was asymmetric. The deformation on the left side was larger than that on the right side. During construction, the tunnel surrounding rock was very fragmented, the rock on the tunnel face was liable to slide along the stratum, the water in the stratum was abundant, and the surrounding rock softened easily by water. These factors made the tunnel construction difficult and had a great risk. Figure 5 shows the deformation and ring breakage of the primary lining.

The no. 2 inclined shaft exhibited large deformation of the surrounding rock from mileage XK0060 to XK1666. According to statistics, the cumulative length of the large deformation section was 1055 m (the average deformation was more than 500 mm), accounting for 58% of the total length of the inclined shaft. The maximum cumulative convergence value of the surrounding rock deformation was 2936 mm, the maximum convergence rate of deformation was 814 mm/d, and the cumulative removal and replacement rate of steel arch was 30%.

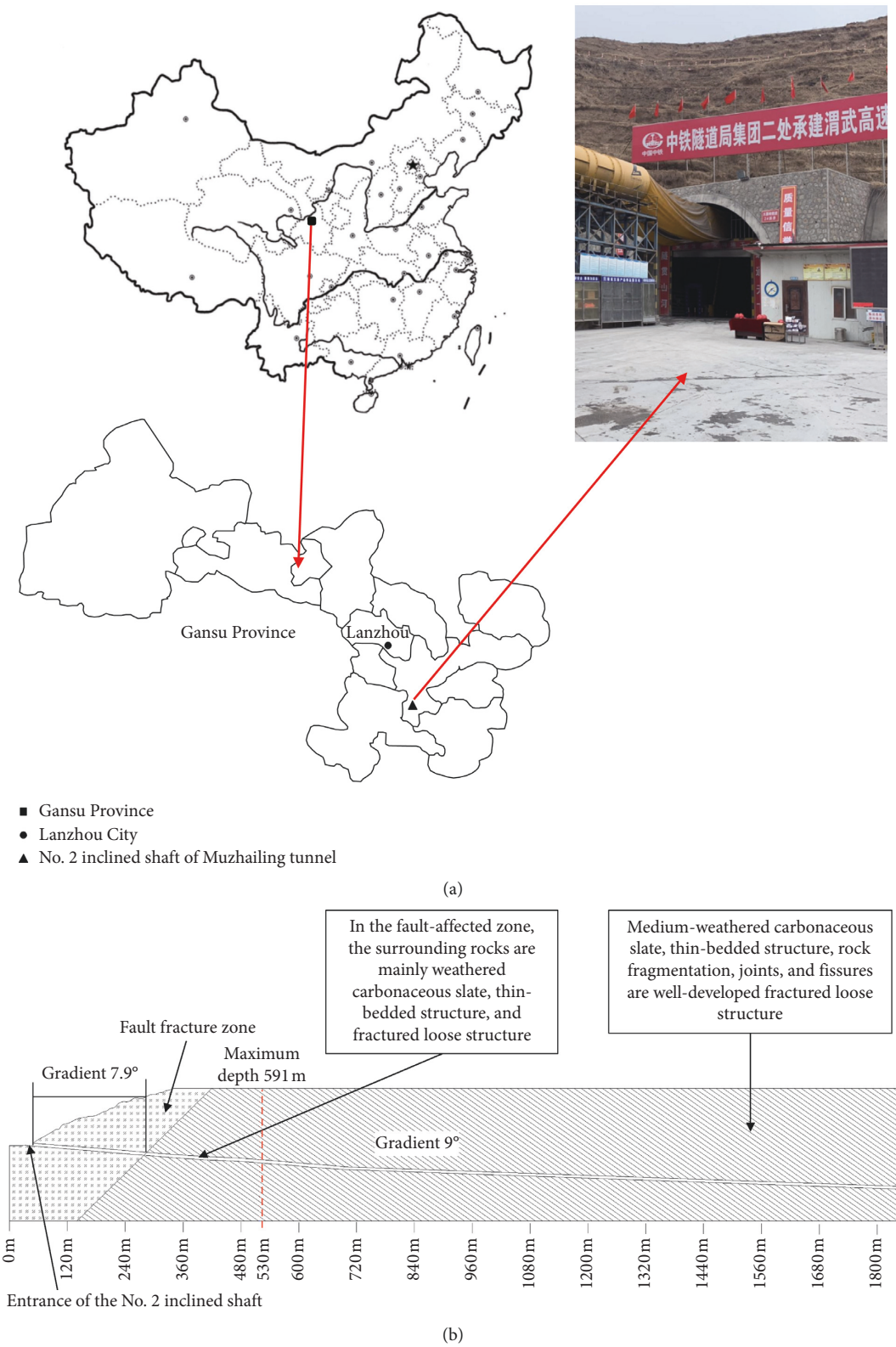


Figure 1: The overview situation of the no. 2 inclined shaft. (a) The geographical location of the no. 2 inclined shaft of the Muzhailing tunnel. (b) The longitudinal section of the no. 2 inclined shaft.

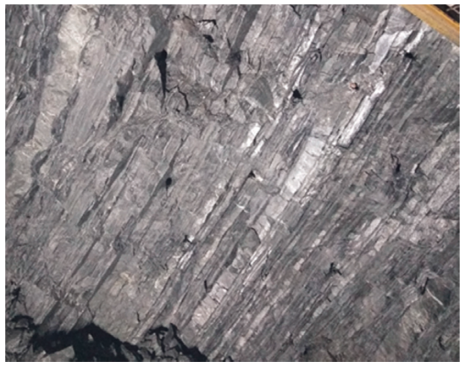

Figure 2: Tunnel exposure of carbonaceous slate.

## 3. Rock Strength under Point Load Strength Test

The surrounding rock of the tunnel was severely weathered, and the joint fissures were well developed. The lithology is mainly carbonaceous slate, which contained a small amount of sandstone. Rock samples were greatly affected by a disturbance in the acquisition, and the standard sample processing was difficult. Therefore, the point load intensity instrument was used for field rapid experiments. The uniaxial compressive strength of the rock was obtained by converting point load into uniaxial strength [8]. The strength of carbonaceous slate and sandstone in the natural state was counted in the range of XK1740 to XK1800. The strength of carbonaceous slate and sandstone after 24 hours of water absorption was also counted. The experimental instruments and some samples are shown in Figure 6.

The test results are shown in Figure 7. Sixty-five samples of carbonaceous slate were selected in the natural state, and the average uniaxial strength was 29.5 MPa. Sixty-five samples of carbonaceous slate were selected after 24 hours of water absorption, and the average uniaxial strength was 11.7 MPa. In the natural state, the average strength of sandstone was 115.12 MPa. After 24 hours of water absorption, the average strength of sandstone was 75.8 MPa.

## 4. NPR Constant Resistance and Large Deformation Anchor Cable Tunnel Support

*4.1. Structure Composition of NPR Anchor Cable.* The NPR anchor cable is a composite device with a unique negative Poisson's ratio structure. As shown in Figure 8, the NPR anchor cable consists of casing pipe, piston-shaped cone body in casing pipe, anchor cable installed on cone body, face pallet, and locking device (Figure 8(a)). When the external load applies to the face pallet, the axial load (pull load) will produce at the free end of the anchor cable. The locking device will lock on the anchor cable and simultaneously push the cone body into the casing pipe. So the casing pipe will displace in the opposite direction to the anchoring end. The movement of the casing pipe is equivalent to the slip of the cone relative to the inner wall of the casing pipe. The small-end diameter of the cone body is slightly smaller than the internal diameter of the casing pipe. The large-end diameter of the cone body is slightly larger than the inner diameter of the sleeve pipe in order to generate the frictional resistance [9]. When the cone body slips in the casing pipe, the casing pipe will produce radial expansion deformation, resulting in negative Poisson's ratio (NPR) structure effect.

*4.2. Installation of NPR Anchor Cable.* Compared with the traditional anchor cable, the NPR anchor cable has one more constant resistance device. In the installation of the anchor cable, a constant resistance device should be installed on the basis of the original hole reaming. The other construction techniques are the same as that of the ordinary prestressed anchor cable. In the process of installing the NPR anchor cable, the pneumatic roof bolter is used to drill anchor cable holes on the surface of the surrounding rock at first. Then use a special reaming drill (Figure 9(a)) to enlarge the drilled hole to install a constant resistance device. After reaming, insert the resin anchoring agent (Figure 9(b)) into the hole and insert the anchor cable immediately. The constant resistance device and pallet are installed while the anchor cable is in place, and the locking device is installed (Figure 9(b)). After the completion of the above process, the pneumatic roof bolter is used to connect the anchor cable end, and the resin anchoring agent in the hole is stirred to uniformly bond the resin anchoring agent with the surrounding rock and the anchor cable (Figure 9(c)). The resin anchoring agent solidifies quickly. Wait for 2 min-3 min to use the hydraulic tensioner to apply pretension force to the anchor cable (Figure 9(d)).

*4.3. Working Principle of NPR Anchor Cable.* NPR rock mass is defined as engineering rock mass supported by the NPR anchor cable [9]. NPR constant resistance and large deformation anchor cable can extend to 1100 mm [10], which can release the deformation energy of the surrounding rock while maintaining the stability of the rock mass and preventing the destruction of the surrounding rock due to large deformation. The interaction between the NPR anchor cable and the surrounding rock can be divided into three steps [11, 12]:

(1) Figure 10(a) shows that the original stable rock mass is destroyed after tunnel excavation. On the one hand, based on stress redistribution, there will be stress concentration in the surrounding rock, resulting in tension zone or plastic zone, so the surrounding rock will produce elastic deformation and plastic deformation. The sum of the energy released by the two kinds of deformation is collectively called the deformation energy $U_D$. On the other hand, due to the loosening of the surrounding rock caused by tunnel excavation and the influence of geological structure, the stability of the surrounding rock is reduced, resulting in displacement of the surrounding rock on the tunnel surface, and the surrounding rock does work to the outside (the work done by the surrounding rock is expressed as $W$). Therefore, it is

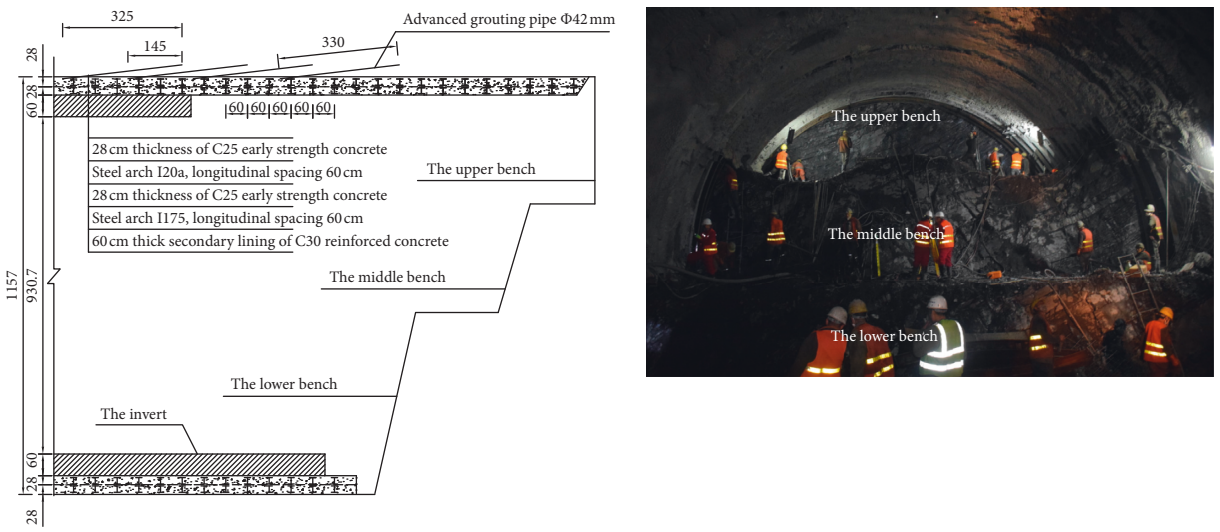


Figure 3: Three-bench excavation form of the tunnel. (a) Longitudinal section support of the tunnel. (b) Real scene of cross section of the tunnel.

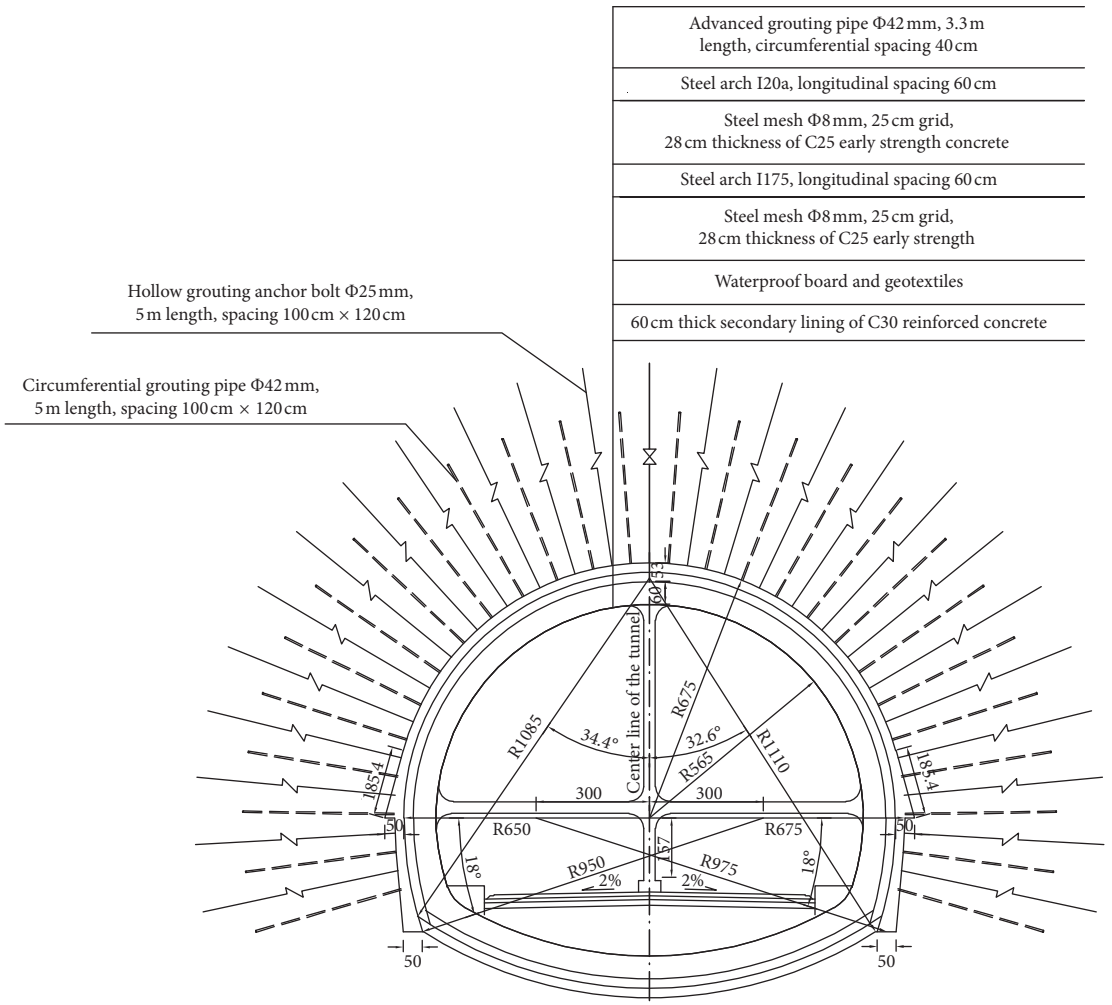


Figure 4: Form of original tunnel support design.


(a) (b)

Figure 5: Deformation and failure characteristics of primary lining. (a) Distortion of steel arch. (b) Large deformation of the surrounding rock.

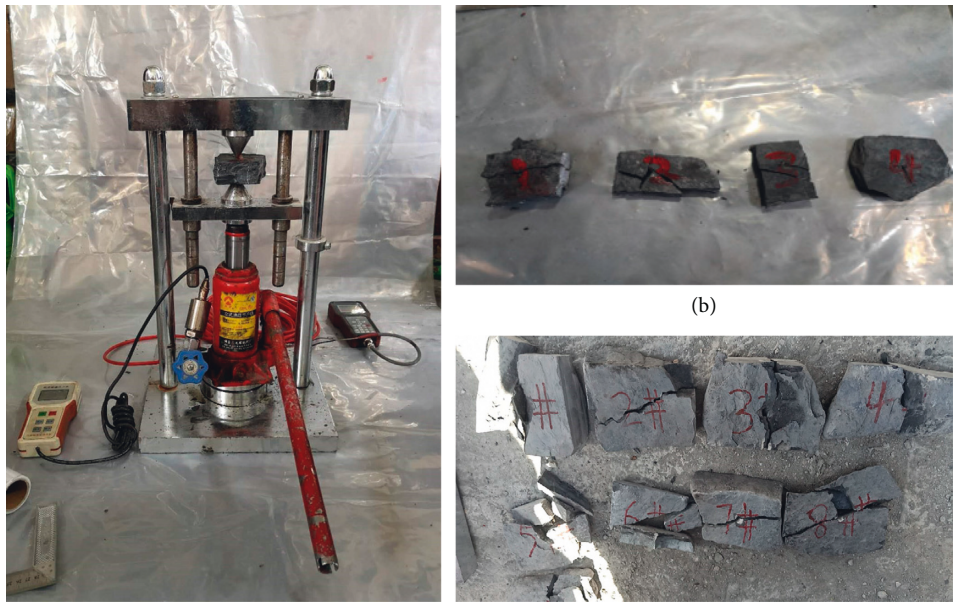

(a) (b) (c)

Figure 6: Laboratory instruments and some samples.

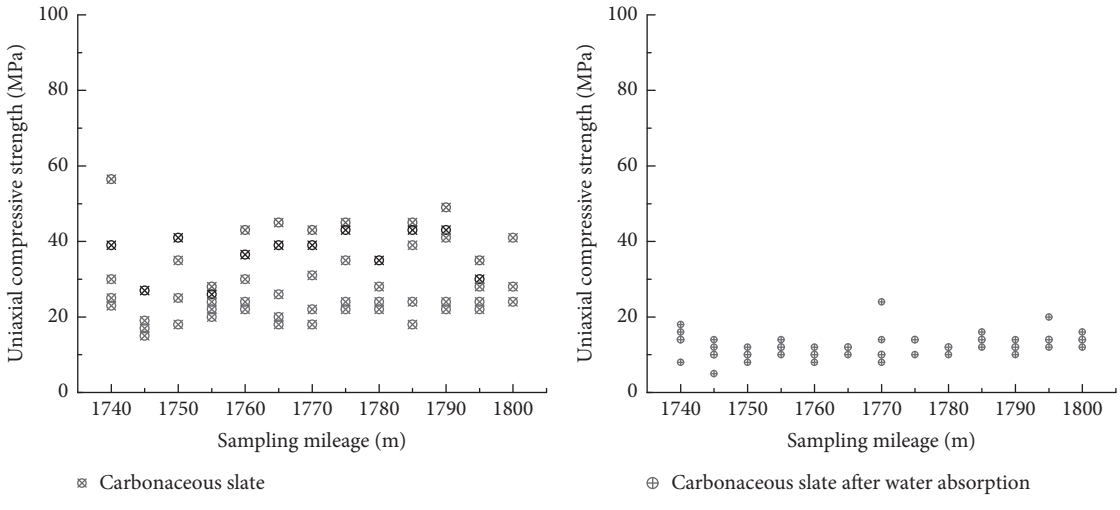


(a) (b)

Figure 7: Continued.

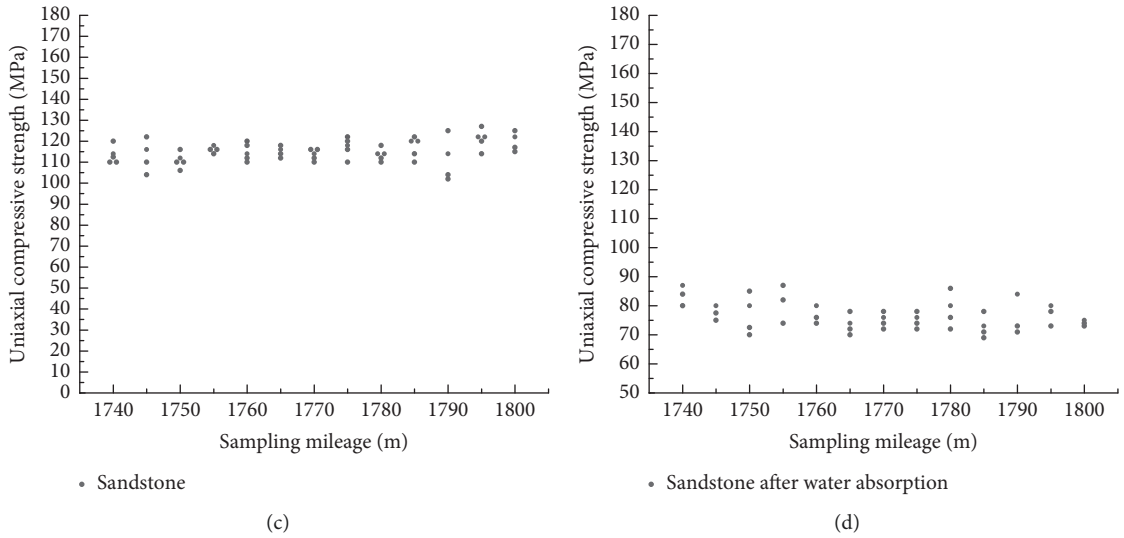


Figure 7: Uniaxial strength of carbonaceous slate and sandstone at different mileage in the no. 2 inclined shaft. Strength of carbonaceous slate (a) in the natural state and (b) after 24 hours of water absorption. Strength of sandstone (c) in the natural state and (d) after 24 hours of water absorption.

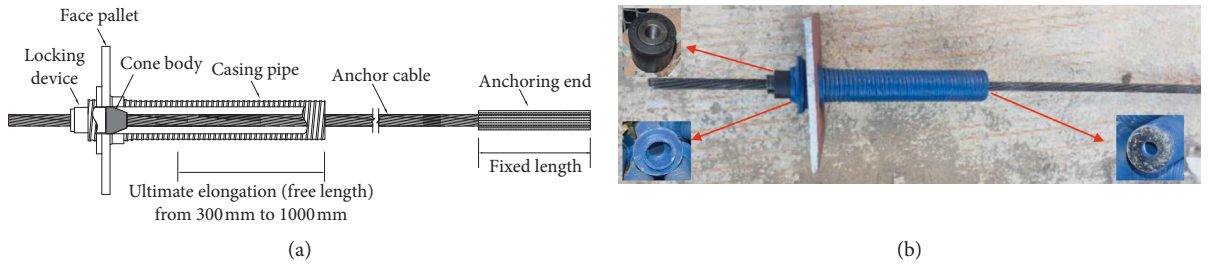


Figure 8: NPR constant resistance and large deformation anchor cable. (a) Composition of the NPR anchor cable. (b) Photos of the NPR anchor cable.

necessary to install the NPR anchor cable to control the surrounding rock deformation before deformation and failure of the deep rock mass.

(2) The energy balance equation of NPR rock mass can be expressed as follows [9]:

$$U = U_D + W. \tag{1}$$

The $U$ in formula (1) is the total potential energy of the surrounding rock. The excess energy $\Delta U$ ($\Delta U$ is the energy absorbed by the NPR anchor cable) in the rock mass is as follows:

$$\Delta U = U - U_D = W. \tag{2}$$

From the energy balance relationship of NPR anchor support in Figure 11, it can be seen that the constant resistance $P_0$ of the NPR anchor cable is known. In the ideal elastic stage, the displacement is $X_0$ when the external load is less than the constant resistance $P_0$. When the external loading is equal to $P_0$ and any displacement $X$ is output, the energy absorbed by a single NPR anchor cable can be expressed as

$$W = \frac{P_0 X_0}{2} + P_0 (X - X_0), \tag{3}$$

where the first $W_0 = P_0 X_0/2$ is the elastic energy absorbed by the elastic deformation of the anchor cable material, and the second $W_Y = P_0 (X - X_0)$ is the energy absorbed by the NPR anchor cable during the structural yield stage. When the number of NPR anchor cables is sufficient enough (the number of NPR anchor cables is $N$), the deformation of the surrounding rock is approximately uniform. Based on formulas (2) and (3), the basic relationship between NPR anchor support system and surrounding rock energy release can be obtained as follows:

$$NP_0 = \frac{2\Delta U}{2X + X_0}. \tag{4}$$

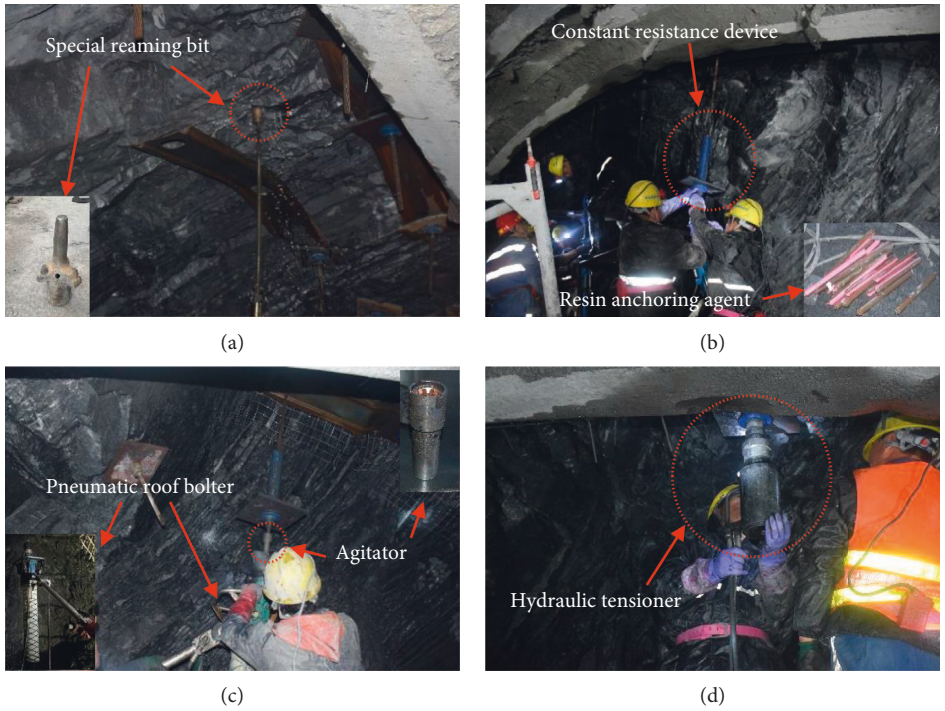


Figure 9: NPR anchor cable installation process. (a) Reaming operation. (b) Installing constant resistance device. (c) Mixing resin anchoring agent. (d) Applying pretension force to the anchor cable.

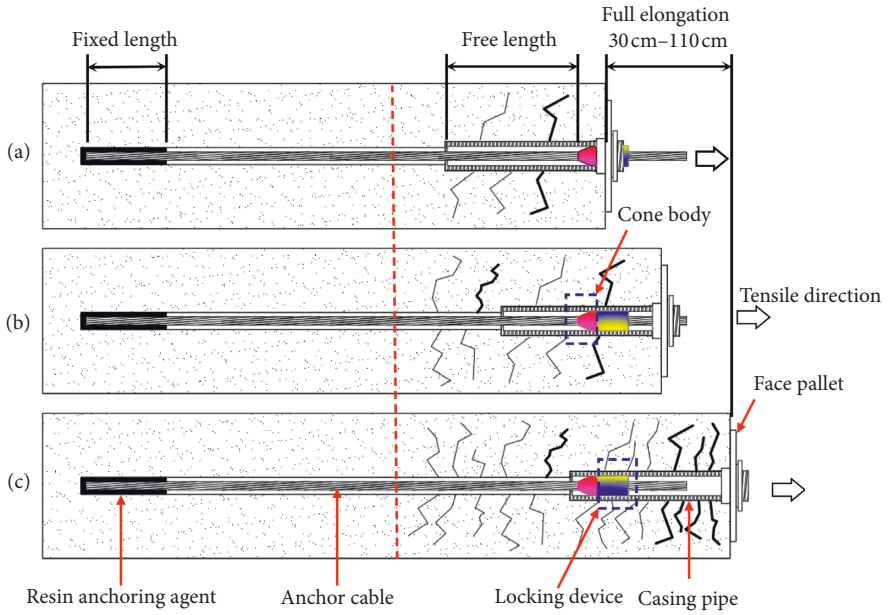


Figure 10: Working principle of the NPR anchor cable. (a) Installation of the NPR anchor cable. (b) Working state when the rock deforms. (c) Rock deformation at full elongation of the NPR anchor cable.

In the process of disturbance instability, creep or large deformation of the surrounding rock, when the loads generated by deformation reach or exceed the constant resistance range of anchor cable design, the cone body inside the NPR anchor cable slips through friction, i.e., the structural deformation of the NPR anchor cable with the deformation of the surrounding rock occurs axial tension and radial expansion to absorb deformation energy, instead of only depending on the material deformation of the anchor cable, thus avoiding the failure of support caused by the breakage of the anchor cable, as shown in Figure 10(b).

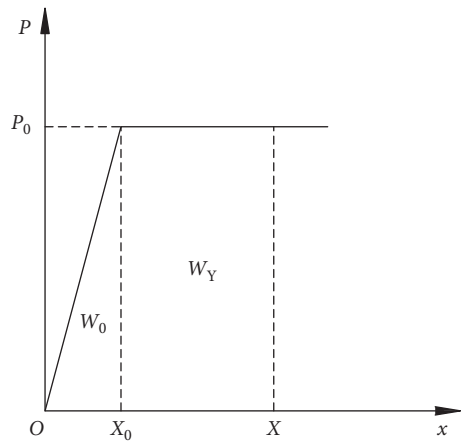


Figure 11: Energy balance relation curve of the NPR rock.

(3) After large deformation of the surrounding rock, the internal stress of the surrounding rock reaches a new balance. When the energy of the surrounding rock deformation is released, the surrounding rock pressure generated by surrounding rock deformation is less than the design constant resistance $P_0$ of the NPR anchor cable, i.e., the axial force of the NPR anchor cable is less than the friction resistance of constant resistance device. At this time, the surrounding rock returns to a stable state again under the support of the anchor cable, as shown in Figure 10(c).

In summary, the NPR anchor cable still has the resistance to deformation after the axial force of the anchor cable is greater than the constant resistance, so the failure phenomenon of sudden fracture will not occur. In tunnels with this new type of anchor cable as supporting material, when the surrounding rock is deformed, the NPR anchor cable will be stretched and released the surrounding rock deformation energy. When the surrounding rock is stabilized again, the NPR anchor cable will maintain stable supporting resistance after the stretching deformation.

*4.4. Design of NPR Anchor Cable Support.* The 100 m inclined shaft no. 2 was selected as the test section of the tunnel. Under the condition that the original technology was unchanged, but the hollow grouting anchor bolt and advanced grouting pipe support, as well as circumferential grouting pipe support, were cancelled, and the original double-deck steel arch frame was replaced by a single-deck one. The support scheme of NPR constant resistance and large deformation anchor cable + W-shaped steel strip + high strength flexible mesh (polyester fiber material) was adopted, and the pretension force of the anchor cable was 350 kN. Because the surrounding rock of the tunnel was in a thin inclined state and the deformation on the left side was large, the asymmetric support was adopted according to the deformation and failure form of the surrounding rock [13, 14]. The form of NPR anchor support is shown in Figure 12.

## 5. Numerical Analysis of NPR Anchor Cable Support

*5.1. Numerical Models and Boundary Conditions.* In this paper, 3DEC (Three-Dimensional Distinct Element Code) discrete element software was used for numerical analysis. As shown in Figure 13, a tunnel excavation model was established, which included tunnel section, uniformly distributed joints, and dominant joints [15]. The geostress of the model was estimated at 500 m depth, the vertical geostress was 12.5 MPa, the maximum horizontal stress was 21 MPa, and the minimum horizontal stress was 12.5 MPa. When the dip angle of the stratum is 45°, the deformation of the surrounding rock is most disadvantageous [16]. Therefore, the dip angle of the model stratum was 45°. Considering the boundary effect caused by excavation, the model was constructed using 3DEC, with a length × width × thickness of 60 m × 60 m × 30 m. The reverse arch at the bottom of the tunnel was filled with concrete. Stress constraints were applied to the model, and fixed constraints were applied to the bottom. Considering the dominant joints and uniformly distributed joints, the deformation characteristics, principal stress distribution characteristics, and plastic zone characteristics of the surrounding rock under NPR anchor cable support and original steel arch support were compared. Finally, the interaction between the anchor cable and the surrounding rock was analyzed.

As shown in Figure 14, the support measures of the anchor cable were asymmetric. The tunnel anchor cable and initial support were constructed according to the actual project. The length of the anchor cable in the initial support was 10 m and 5 m, and the pretension force was 350 kN. The thickness of the shotcrete and steel arch was 25 cm, and the height of the inverted arch was 2 m. The elastic modulus of the primary lining was 28.8 GPa. The Mohr–Coulomb constitutive model was used for the rock, and the Coulomb slip model was used for joints. In addition to the dominant joint group, other fractures had local anisotropic characteristics, but macroscopically they were regarded as isotropic. Continuous medium equivalence was carried out by using the method of 3DEC-Trigon [17]. In the process of equivalence, the REV characteristics of the rock mass [18], the transformation from rock to rock mass parameters [19, 20], and the selection of joint parameters should be considered [21]. The rock strength parameters and mechanical parameters of carbonaceous slate are shown in Tables 1 and 2.

*5.2. Comparative Analysis of Surrounding Rock Deformation.* As shown in Figures 15 and 16, the surrounding rock displacement nephrograms of steel arch support and anchor support are shown, respectively. In order to clearly compare the deformation of the surrounding rock and initial support in different stages and different supporting conditions, the same color scale is selected for nephrogram analysis. In the process of calculation, the displacement of two points was monitored. The green monitoring line represents the left side at the junction of the upper bench and the middle bench, and

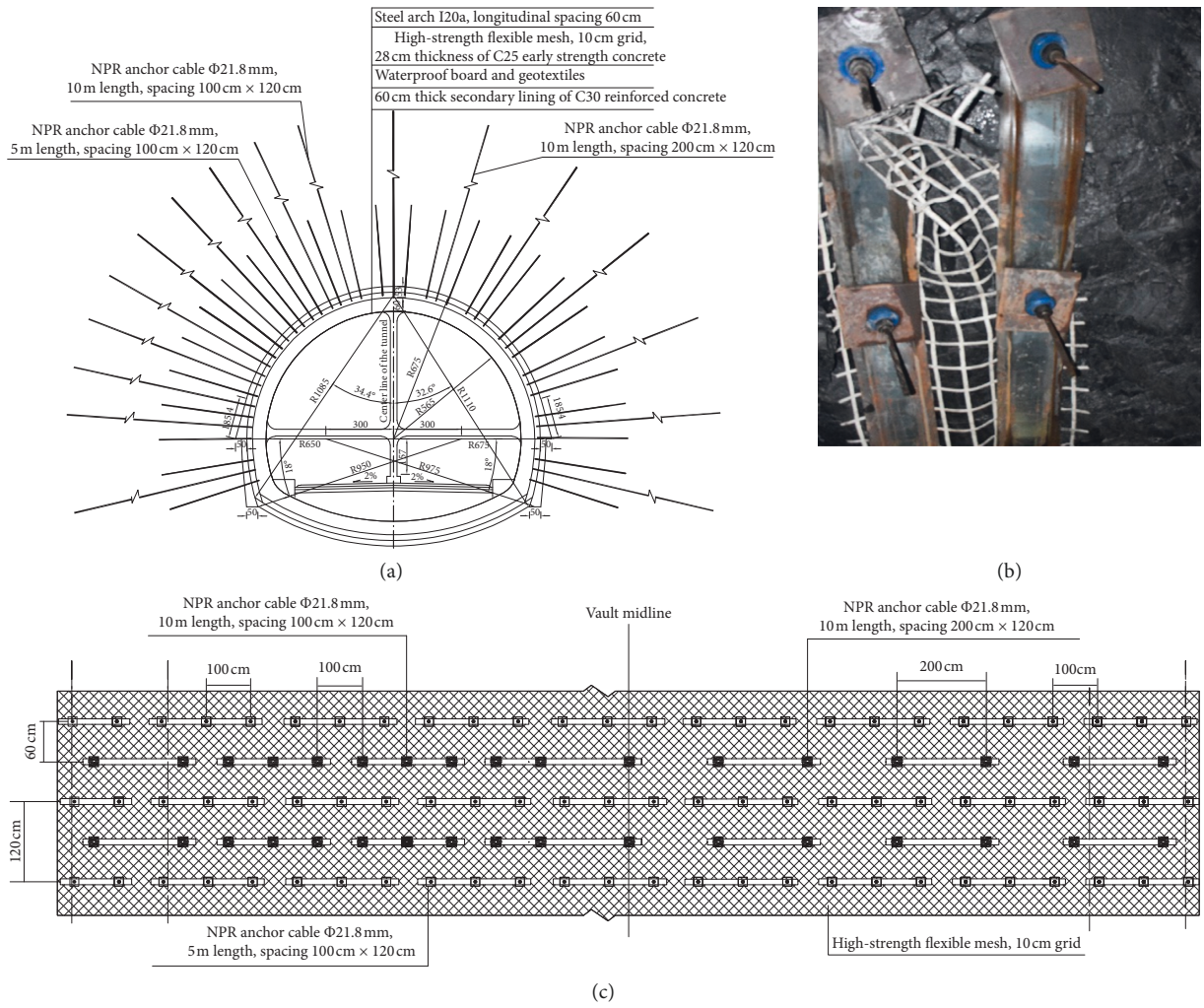


Figure 12: NPR anchor cable support in the tunnel. (a) Cross section of the tunnel supported by the NPR anchor cable. (b) Photo of the NPR anchor cable support. (c) Tunnel annular arrangement of the NPR anchor cable.

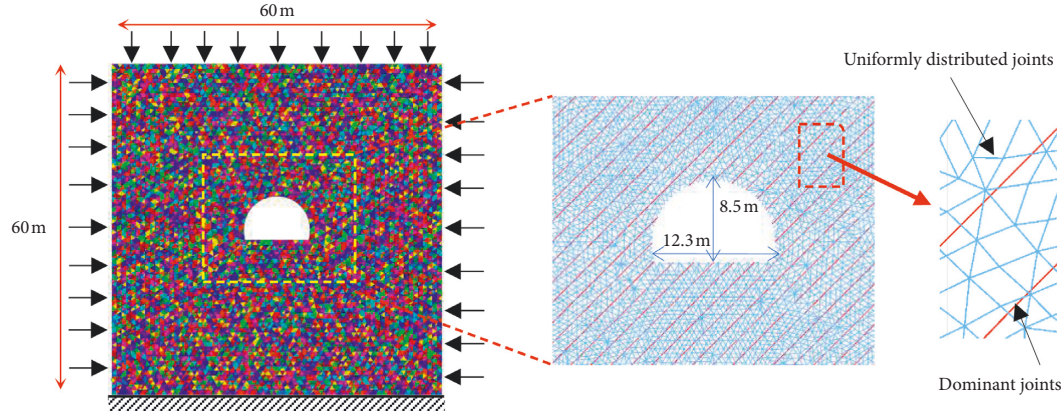


Figure 13: Numerical computation model.

the red monitoring line indicates the same position on the right side. When calculating to 1000 steps, the asymmetry of surrounding rock deformation was not obvious under two supporting measures (Figures 15(a) and 16(a)). When calculating to 2000 steps, the maximum displacement of the monitoring point on the left side was 0.28 m and that on the right side was 0.22 m under the support of the steel arch, which resulted in the phenomenon of asymmetric

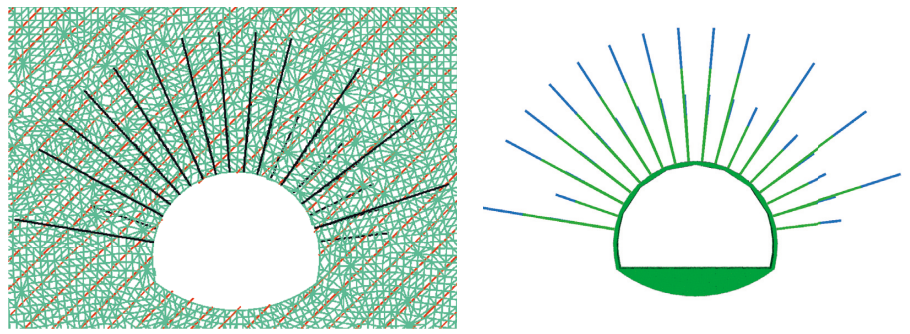

(a) (b)

Figure 14: Anchor cable arrangement in the tunnel. (a) Anchor cable and surrounding rock. (b) Anchor cable and lining.

Table 1: Rock properties and rock mass properties.

| Lithology | Rock | | GSI | Constant | | | | Rock mass | |
|---|---|---|---|---|---|---|---|---|---|
| | $\sigma_{ci}$ (MPa) | $E_i$ (GPa) | | $m_i$ | $m_b$ | **S** | $a$ | $\sigma_{cmass}$ (MPa) | $E_{rm}$ (GPa) |
| Natural state carbonaceous slate | 29.5 | 7.6 | 40 | 19 | 1.091 | 0.000335 | 0.511 | 7.4 | 0.6 |

Table 2: Parameters for the rock mass.

| Lithology | Density (kg/m$^3$) | Block properties | | | | | Structural plane properties | | | | |
|---|---|---|---|---|---|---|---|---|---|---|---|
| | | $K$ (GPa) | $G$ (GPa) | $C^b$ (MPa) | $\varphi^b$ | $\sigma_t^b$ (MPa) | $K^n$ (GPa) | $k^s$ (GPa) | $C^j$ (MPa) | $\varphi^j$ | $\sigma_t^j$ (MPa) |
| Natural state carbonaceous slate | 2500 | 0.44 | 0.25 | 1.7 | 22 | 0.6 | 30.21 | 12.08 | 3.75 | 29 | 3.45 |

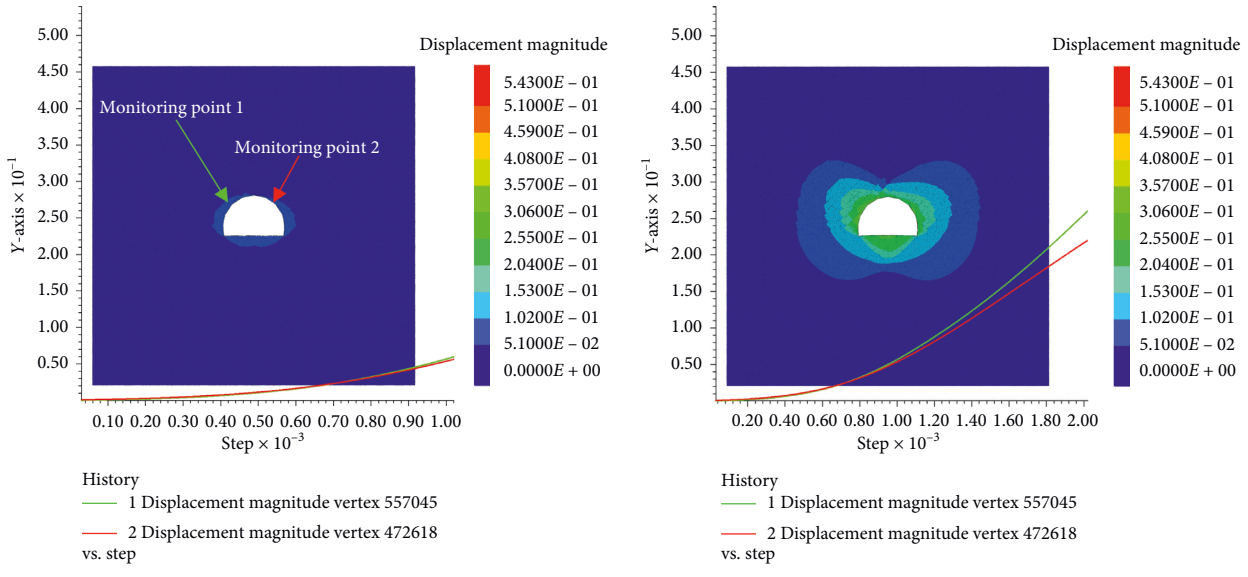


(a) (b)

Figure 15: Continued.

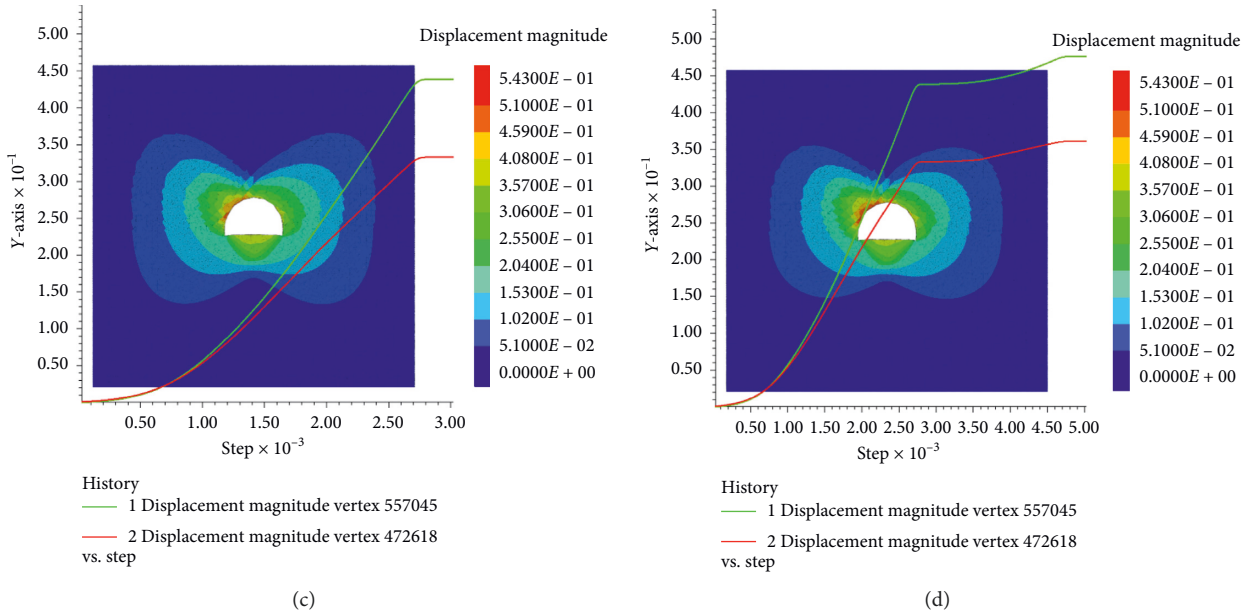


Figure 15: Surrounding rock displacement nephrogram with the steel anchor support. (a) Step 1000, (b) step 2000, (c) step 2700, and (d) step 5000.

deformation (Figure 15(b)). Under the anchor cable support, the displacement of the surrounding rock at the left monitoring point was 0.011 m and that at the right side was 0.012 m, which showed that the asymmetric deformation of the tunnel was not obvious (Figure 16(b)). The displacement of the surrounding rock tended to be stable under two kinds of support measures when the calculation was about 2,700 steps (Figures 15(c) and 16(c)). Finally, the maximum displacement of the monitoring point on the left side was 0.49 m and that on the right side was 0.33 m under the steel arch support, which indicated that the deformation of the surrounding rock presented obvious asymmetry (Figure 15(d)). Under the anchor cable support, the maximum deformation of the left monitoring point was 0.19 m and that on the right side was 0.17 m. Compared with the steel arch support, the asymmetric deformation of the surrounding rock under the anchor support was still not obvious (Figure 16(d)). In summary, the anchor cable support under asymmetric arrangement can effectively control the deformation of the surrounding rock and effectively alleviate the asymmetric deformation caused by surrounding rock structure and geostress.

*5.3. Comparative Analysis of Shear Stress Characteristics.* The distribution of shear stress under the steel arch support and anchor cable support is shown in Figure 17. In the process of calculation, the shear stress concentration area of tunnel surrounding rock was continuously transferred to the deep under two supporting measures, respectively. After the stability of the surrounding rock supported by steel arch (Figure 17(a)), the maximum shear stress on the left side of the surrounding rock was 6.5 MPa and that on the right side was 6.38 MPa. The shear stress concentration area was asymmetrical. The shear stress concentration area on the left upper was obviously larger than that on the right upper. The maximum shear stress in the upper left was located at a depth of 7.9 m in the surrounding rock and 6.6 m deep in the upper right. Under the support of anchor cables (Figure 17(b)), the asymmetry phenomenon in the shear stress concentration area of the surrounding rock was reduced, but the maximum shear stress was obviously higher than that of the surrounding rock supported by steel arch. The maximum shear stress on the left side was 7.4 MPa, the maximum shear stress on the right side was 7.2 MPa, the maximum shear stress on the left upper was located at a depth of 1.6 m in the surrounding rock, and the maximum shear stress on the right upper was located at a depth of 2.2 m in the surrounding rock. Under the control of the anchor cable, the shear resistance of the surrounding rock was obviously improved.

*5.4. Characteristics of Plastic Zone.* According to the analysis of the plastic zone development under the steel arch support and anchor cable support shown in Figure 18, it can be seen that the failure of the plastic zone of the surrounding rock was mainly a shear failure, and there was a phenomenon of shear failure and tensile failure coexisting in the shallow part of the surrounding rock. Compared with the steel arch support (Figure 18(a)), the plastic zone area at the junction of upper and lower benches was obviously reduced under the support of anchor cables (Figure 18(b)), but the plastic zone area was not much different at the bottom of the tunnel due to the absence of the anchor cable support.

*5.5. Interaction between NPR Anchor Cable and Surrounding Rock.* Figure 19 shows the prestress diffusion effect of combined support with 5 m and 10 m anchor cables under the prestress force (350 kN) and the stress condition of

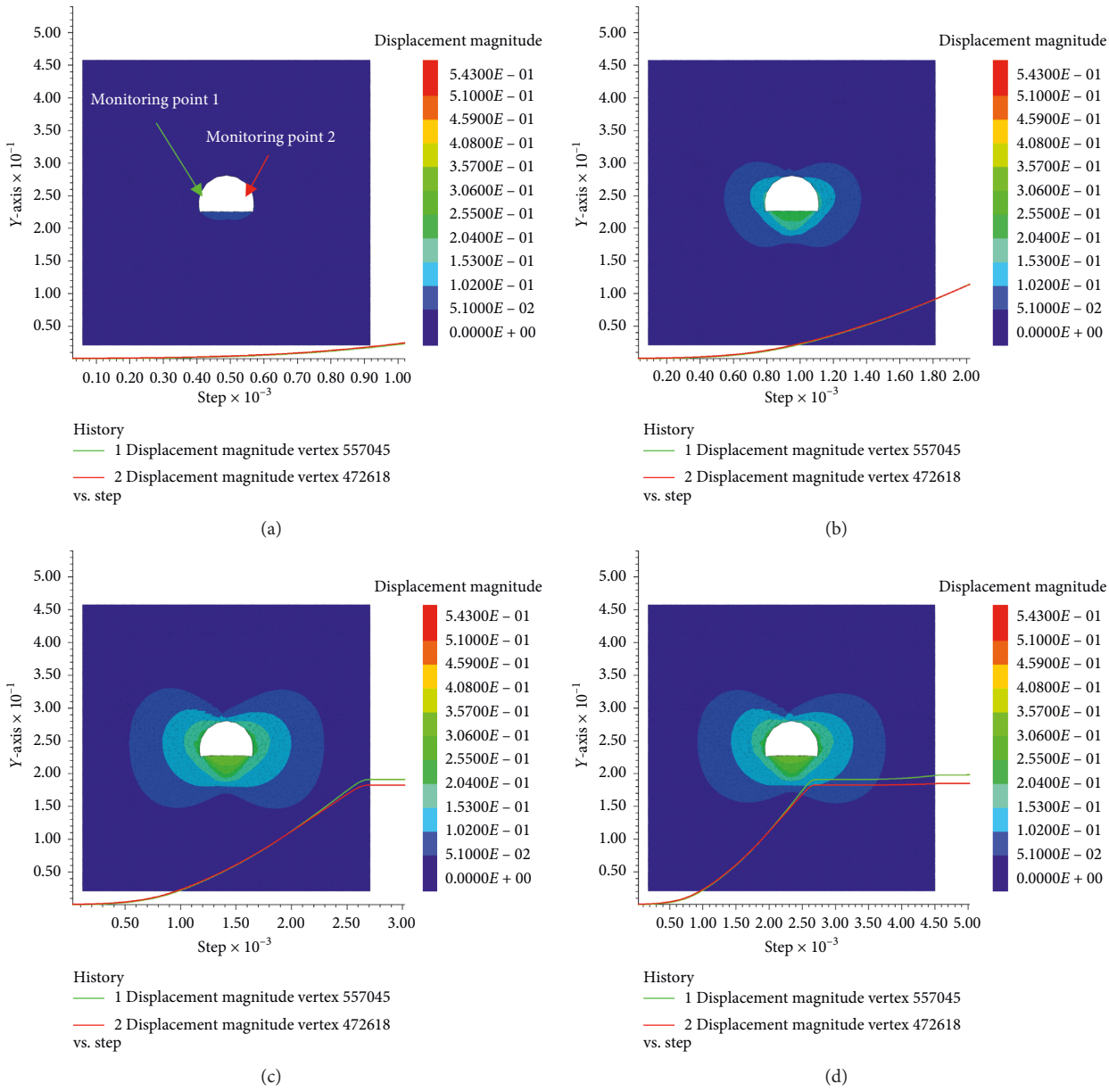


Figure 16: Surrounding rock displacement nephrogram with the anchor cable support. (a) Step 1000, (b) step 2000, (c) step 2700, and (d) step 5000.

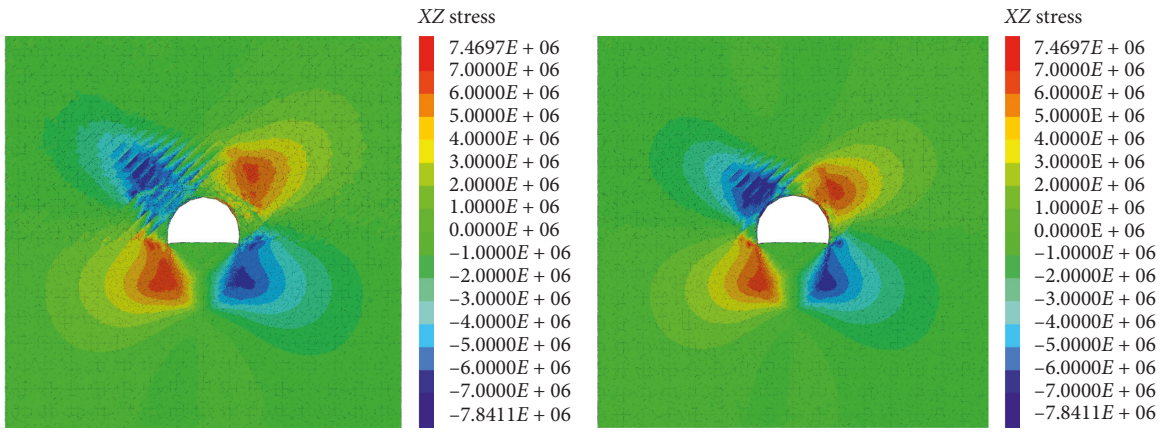


Figure 17: Shear stress nephrogram of the surrounding rock. (a) Surrounding rock shear stress nephrogram with the steel arch support. (b) Surrounding rock shear stress nephrogram with the anchor cable support.

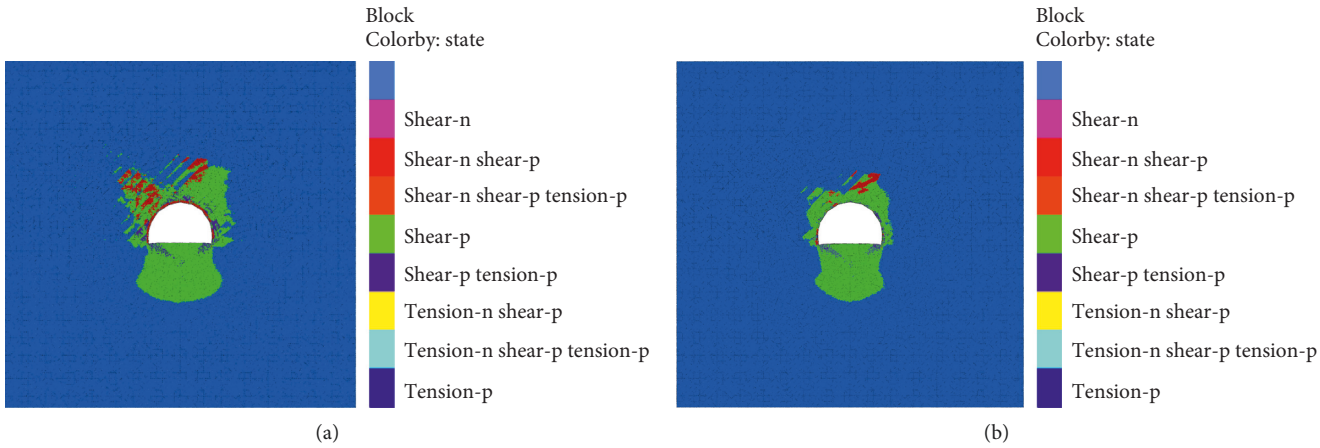


Figure 18: Distribution characteristics of the plastic zone of the surrounding rock. Surrounding rock distribution of the plastic zone with (a) the steel anchor support and (b) the anchor cable support.

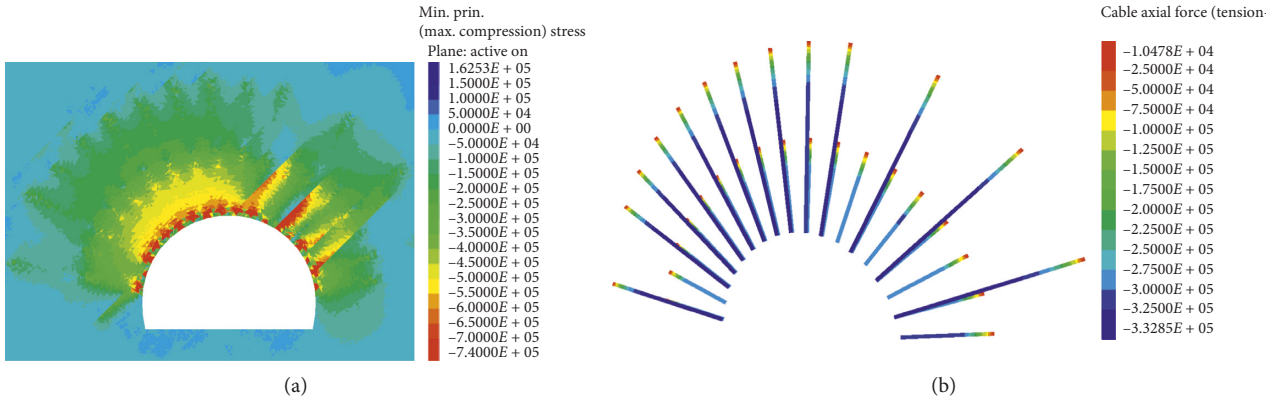


Figure 19: Long and short anchor cables under preloading 350 kN. (a) Diffusion effect of anchor cable prestress. (b) Stress of the anchor cable.

anchor cables. The left shoulder of the tunnel was prone to large deformation and failure, so 5 m anchor cables were evenly distributed (1 m annular spacing) and 10 m anchor cables were asymmetrically arranged (1 m annular spacing at the left shoulder and 2 m annular spacing at other parts). Because of the combination of long and short anchor cables, the stress in the supporting area was significantly increased. The maximum stress on the rock surface is 0.74 MPa, the stress at the anchor end of 10 m anchor cable is 0.19 MPa, and the stress at the anchor end of 5 m anchor cable is 0.4 MPa (Figure 19(a)). The prestress was effectively diffused within 10 m of the surrounding rock. Under the superposition of effective stress produced by long and short anchor cables, the fan-shaped prestressing extension area was formed in the surrounding rock, and the 10 m anchor cables were the fan-shaped skeleton. Long and short anchor cables could produce better active control effect on the surrounding rock under high prestress force. The prestress force at the end of 10 m anchor cable was 332 kN, and the prestress loss was 18 kN. The end prestress force of 5 m anchor cable was 260 kN, and the prestress loss was 90 kN, as shown in Figure 19(b). Although the anchor cable had a prestress loss, it still maintained a high level.

## 6. Field Test Analysis

*6.1. Field Test Project.* The field monitoring projects of the Muzhailing tunnel cross section include the NPR anchor cable force monitoring, surrounding rock displacement measurement, steel arch internal force monitoring, and surrounding rock deep displacement monitoring. The mileage XK1770 of the no. 2 inclined shaft was selected as a typical monitoring cross section, and the specific location is shown in Figure 20. The purpose of field monitoring is to study the effect of the NPR anchor cable support on the deformation control of the tunnel surrounding rock [22]. The installation of field monitoring equipment is shown in Figure 21.

*6.2. Internal Force Analysis of Steel Arch.* The internal force of steel arch was monitored by the NZS-FBG-SSG strain gauge.

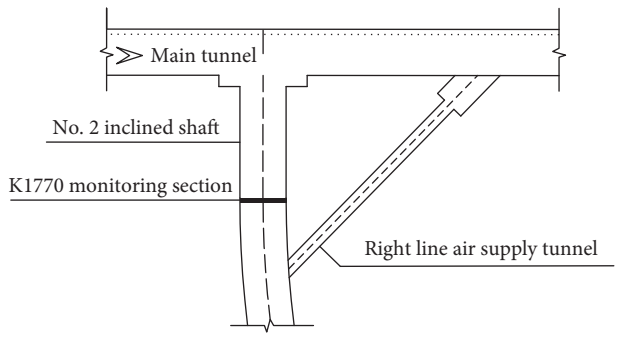


Figure 20: Monitoring section position.

(a) (b) (c)

Figure 21: Installation of field testing equipment. (a) Anchor cable dynamometer. (b) Steel arch strain gauge. (c) Multipoint displacement meter.

Five monitoring points were arranged in the tunnel cross section, and the monitoring results are shown in Figure 22(a). The stress of the steel arch increased with time. After the erection of the upper bench steel arch, the stress of the steel arch increased sharply, and the stress of the left arch shoulder increased fastest. The maximum stress of the steel arch on the left arch shoulder was 208 MPa, but less than maximum ultimate bending stress (215 MPa) of the steel arch. Due to the suspension of the steel arch of the upper bench after the excavation of the middle bench, the stress of the steel arch decreased and then increased slowly with the deformation of the surrounding rock. The stress of the steel arch gradually stabilized after the closure of the steel arch.

*6.3. Convergence Deformation Analysis of Surrounding Rock.* The Leica TS06PLUS-2R500 total station was used to measure the daily deformation of the surrounding rock. Figure 22(b) shows the displacement of the crown, two arch shoulders, and two side walls. From the upper bench excavation stage to the lower bench excavation stage (0–15 days), the surrounding rock was in a period of rapid deformation. The average displacement rates of measuring points A, B, and C were 5 mm/d, 12 mm/d, and 8 mm/d, respectively. The deformation of the surrounding rock in this stage had the characteristics of fast speed and long duration, which were caused by stress redistribution after tunnel excavation. The surrounding rock was in a period of slow deformation from lower bench excavation to the completion of inverted arch construction (15–24 days). The average displacement rates of measuring points A, B, and C were 1.3 mm/d, 3 mm/d, and 2.5 mm/d, respectively. The displacement rates in this period were small, indicating that the surrounding rock was in a stable deformation stage. The displacement of the two measuring points of the tunnel side walls D and E is small. During the monitoring process, after the inverted arch construction, the deformation tended to be stable in about 29 days, showing the asymmetric deformation characteristics of the left side settlement larger than the right side. The maximum deformation of the left arch shoulder and the right arch shoulder is 223 mm and 151 mm, respectively, with 72 mm discrepancy. However, the gap between the two was not very large, indicating that the asymmetric support of the NPR anchor has played a significant role.

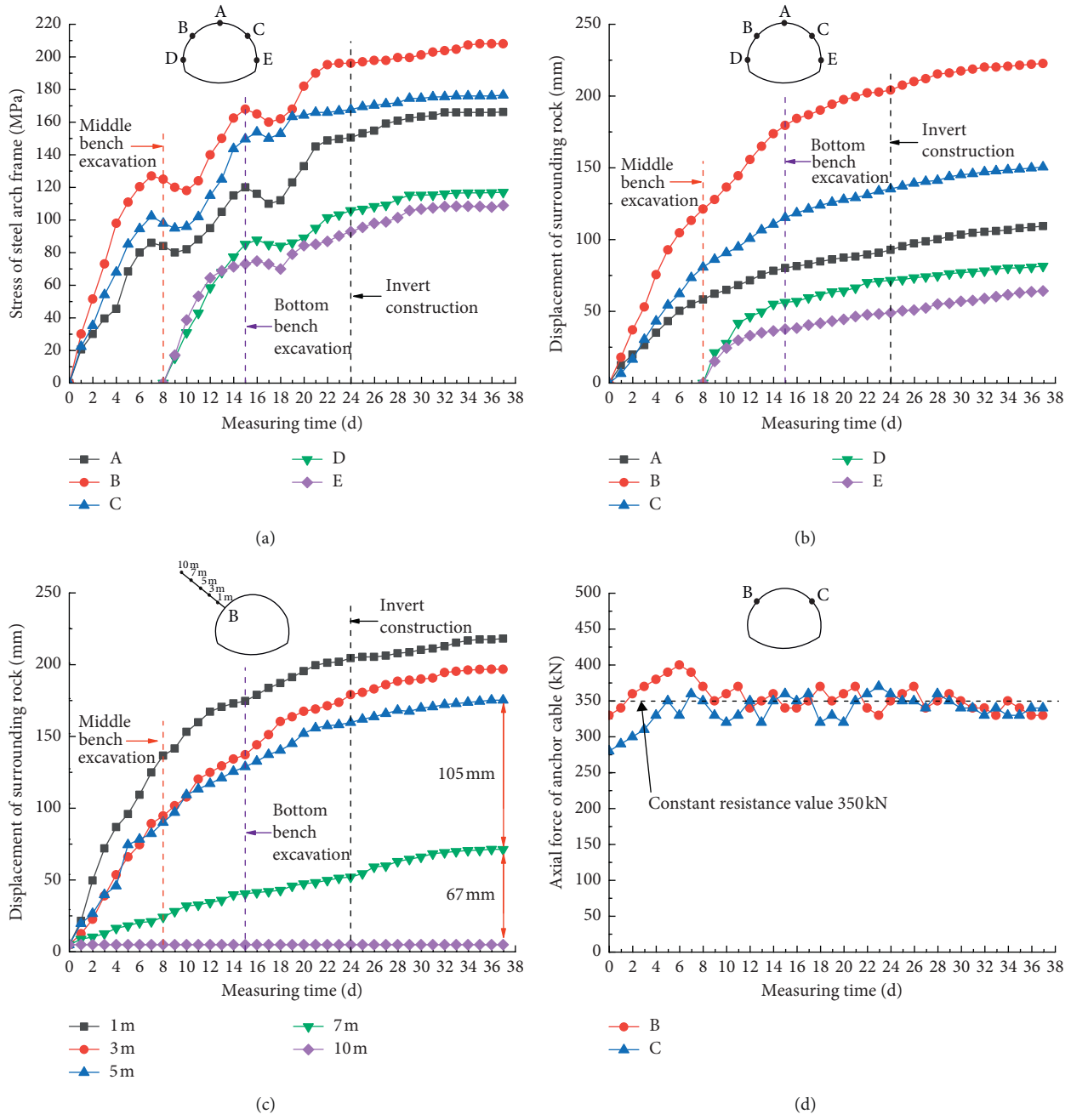


Figure 22: Field test results. Time-history curve of (a) steel arch internal force, (b) surrounding rock displacement, (c) surrounding rock deep displacement, and (d) anchor cable force.

*6.4. Deep Displacement Analysis of Surrounding Rock.* The NZS-FBG-DPG multipoint displacement meter was installed at the depth 1 m, 3 m, 5 m, 7 m, and 10 m away from the surface of the surrounding rock, respectively. The displacement meter was installed at the left arch shoulder (point B of the cross section) where the cross section was most deformed for testing and analysis. The monitoring results of the surrounding rock deep displacement are shown in Figure 22(c).

Under the NPR anchor cable support system, the deformation trend of each depth measurement point was basically the same. The displacement decreased gradually from the surface of surrounding rock to the depth of the surrounding rock. The displacement of the surrounding rock at 1 m on the left arch shoulder was the largest with 202 mm. The deformation of the deep surrounding rock at 10 m was basically 0 mm. Under the control of 5 m NPR anchor cable, the abscission layer of the surrounding rock is smaller in the range of 0–5 m, and it was mainly concentrated between 5–7 m and 7–10 m. The abscission layers range of 5–7 m and 7–10 m were 67 mm and 105 mm, respectively. It shows that the surrounding rock within 5 m forms a pressure-bearing

Table 3: Comparison of numerical simulation and field test.

| Engineering condition | Method | Plastic regions (m) | Force of anchor cable (kN) |
|---|---|---|---|
| NPR anchor cable support | Simulation | 7.5 | 332 |
| | Field test | <10 | 330 |

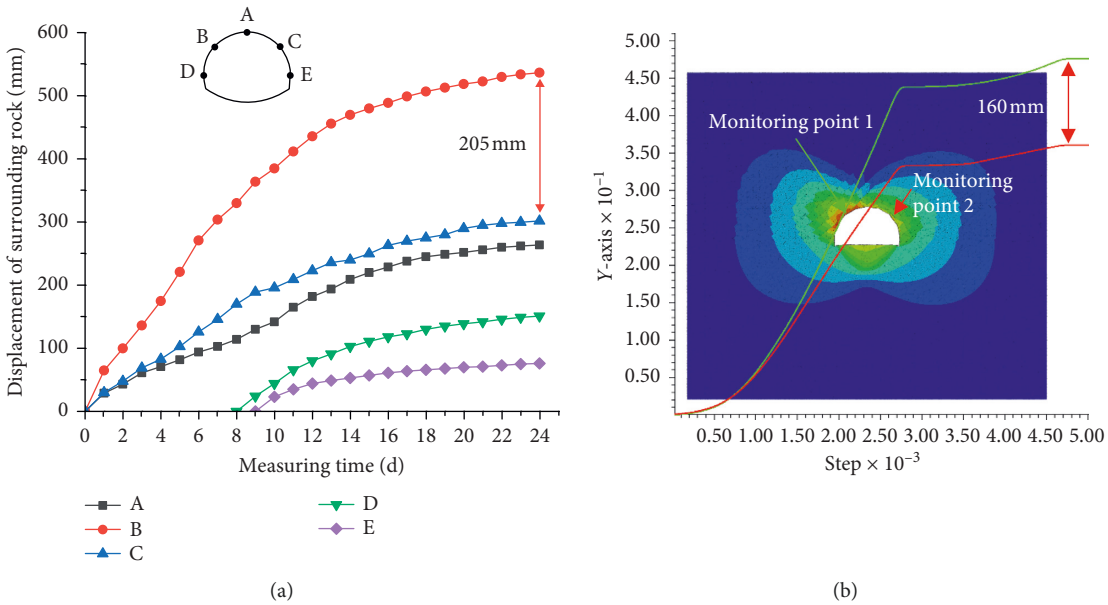


Figure 23: (a) Field test results. (b) Numerical simulation results.

arch under the action of NPR anchor cables, and the 10 m anchor cables play the role of suspension. Both of them work together to control the deformation of the surrounding rock.

*6.5. Force Analysis of NPR Anchor Cable.* The NZS-FBG-ALG anchor cable dynamometers were installed at the end of 10 m anchor cables, which were located at the left and right shoulders of the tunnel cross section. The prestress force applied to the NPR anchor was 350 kN. The test results of the anchor cable axial force are shown in Figure 22(d). Due to the prestress loss, the axial force of the anchor cable at the left anchor shoulder was 330 kN and that of the right arch shoulder was 280 kN. The axial force increased with the increase of the deformation of the surrounding rock. The axial force fluctuated between 340 kN and 370 kN after reaching its constant resistance value (350 kN). After a period of time, the axial force tended to be stable and fell below the constant resistance value, which indicated that the surrounding rock pressure was basically stable.

## 7. Comparative Analysis of Numerical Simulation and Field Test

The influence depth of the plastic zone and the axial force of the anchor cable under the NPR anchor cable support were analyzed by numerical simulation and the field test. The surrounding deformation characteristics of the tunnel supported by steel arch and NPR anchor cable were also analyzed.

The prestress force applied to the anchor cable was 350 kN. As shown in Table 3, the numerical simulation and field test results show that the axial force of the anchor cable was basically the same, and the prestress loss was basically the same. According to the monitoring data of field multipoint displacement meter, the abscission layer of the surrounding rock was less than 10 m, and it can be inferred that the influence range of the plastic zone of the surrounding rock was less than 10 m. The range of the plastic zone calculated by numerical simulation was slightly smaller than that of field monitoring.

Figure 23 shows the analysis results about the deformation of the surrounding rock of the tunnel cross section XK1720. The cross section adopted steel arch support measures. The deformation of the surrounding rock presented the characteristics of asymmetric deformation. The deformation on the left side was larger than that on the right side, which was the same as the numerical simulation results. The deformation of the left shoulder and the right arch shoulder measured in the field was 537 mm and 332 mm, respectively, with 205 mm discrepancy. The deformation of the left shoulder and the right shoulder calculated by numerical simulation was 490 mm and 330 mm, respectively, with 160 mm discrepancy. The numerical simulation results were slightly smaller than the field measurements.

Under the NPR anchor support, Figure 24 shows the analysis results of the XK1770 cross section. Both numerical simulation and field test results show that the large deformation of the surrounding rock decreased obviously, and

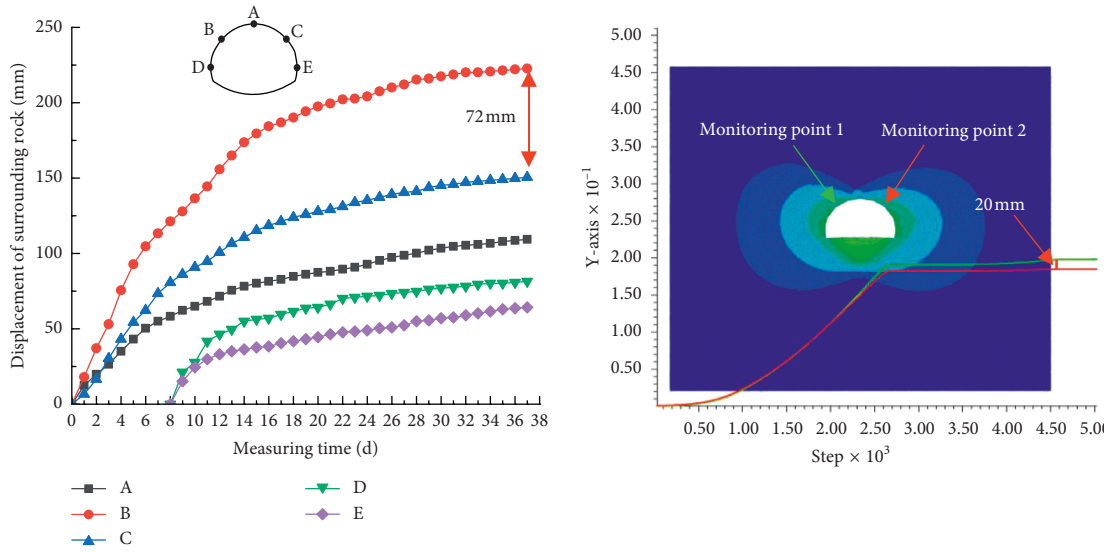


(a) (b)

Figure 24: (a) Field test results. (b) Numerical simulation results.

the deformation on the left side is slightly larger than that on the right side, but the asymmetric deformation was obviously controlled. The difference of deformation between the left and right sides of the tunnel was 72 mm, and the result of numerical simulation was 20 mm. The maximum deformation of the surrounding rock measured in the field was 223 mm, and that calculated by numerical simulation was 190 mm, which shows that the results of the two methods were close to each other.

In summary, the numerical simulation results are close to the field monitoring test results, so the numerical simulation results are effective, which can provide a reference for the selection of support parameters, and the NPR constant resistance and large deformation anchor cable support can effectively control the surrounding rock deformation of large cross-section tunnel.

## 8. Conclusion

This paper introduced the application of NPR constant resistance and large deformation anchor cable support system in tunnels, using 3DEC numerical simulation and field test to study the control effect of the NPR anchor cable on surrounding rock deformation. The following conclusions can be drawn:

(1) The results of numerical simulation analysis show that the asymmetric deformation of the tunnel surrounding rock was obviously reduced under the NPR anchor support, and the deformation of the surrounding rock was less than that of the steel arch support. Under the support of the steel arch, the shear stress concentration area of the tunnel surrounding rock migrates to the depth of the surrounding rock, but under the support of the NPR anchor cable, the shear stress concentration area migrated less to the depth of the surrounding rock, which indicates that the NPR anchor cable support can improve the shear resistance of the surrounding rock. The NPR anchor cable had a better control effect on the development of the plastic zone of the surrounding rock. After the 350 kN prestress force was applied to the anchor cable, although the prestress loss of the anchor cable existed, the stress field generated by long and short NPR anchor cables under high prestress can effectively cover the surrounding rock of the tunnel within the support area and can play an active role in strengthening the surrounding rock of the tunnel.

(2) The field test results show that the displacement of the tunnel surrounding rock converged to a steady state in about 29 days. The deformation of the surrounding rock on the left side was larger than that on the right side, but the maximum displacement and the asymmetry of deformation were obviously reduced compared with before. The prestress force of the NPR anchor cable basically met the design requirement of 350 kN. In the later stage, the force of the anchor cable was maintained at about 330 kN due to the constant resistance of the NPR anchor cable. There was also a significant imbalance in the stress of the steel arch. The stress on the left side of the steel arch was greater than that on the right side, but both were below the ultimate strength of the steel arch. Under the support of the NPR anchor cable, the deep separation zone of the surrounding rock was less than 10 m. Under the action of high prestress of 5 m NPR anchor cable, the abscission layer of the surrounding rock within 5 m was smaller, and the abscission layer range mainly concentrated within 5 m to 10 m of the deep surrounding rock.

(3) According to numerical simulation analysis and field monitoring results, it is proved that under the action of high pretension force to the NPR anchor cable support system, the large deformation problem of initial support of the tunnel surrounding rock can be effectively controlled, which can provide a reference for similar projects in the future.

## Data Availability

The data used to support the findings of this study are available from the corresponding author upon request.

## Conflicts of Interest

The authors declare that they have no conflicts of interest.

## Acknowledgments

Many thanks are due to Gansu Changda Highway Co., Ltd. and Erchu Co., Ltd. of China Railway Tunnel Group for their help and support with the authors.

## References

[1] E. Hoek, P. G. Marinos, and V. P. Marinos, "Characterisation and engineering properties of tectonically undisturbed but lithologically varied sedimentary rock masses," *International Journal of Rock Mechanics and Mining Sciences*, vol. 42, no. 2, pp. 277–285, 2005.

[2] M. A. Meguid and R. K. Rowe, "Stability of D-shaped tunnels in a MohrCoulomb material under anisotropic stress conditions," *Canadian Geotechnical Journal*, vol. 43, no. 3, pp. 273–281, 2006.

[3] D. Brox and H. Hagedorn, "Extreme deformation and damage during the construction of large tunnels," *Tunnelling and Underground Space Technology*, vol. 14, no. 1, pp. 23–28, 1999.

[4] J. Lai, X. Wang, J. Qiu, J. Chen, Z. Hu, and H. Wang, "Extreme deformation characteristics and countermeasures for a tunnel in difficult grounds in southern Shaanxi, China," *Environmental Earth Sciences*, vol. 77, no. 19, pp. 23–28, 2018.

[5] W. Guojun, C. Weizhong, T. Hongming, J. Shanpo, Y. Jianping, and T. Xianjun, "Numerical evaluation of a yielding tunnel lining support system used in limiting large deformation in squeezing rock," *Environmental Earth Sciences*, vol. 77, no. 12, 2018.

[6] D. Merlini, D. Stocker, M. Falanesca, and R. Schuerch, "The Ceneri base tunnel: construction experience with the southern portion of the flat railway line crossing the Swiss Alps," *Engineering*, vol. 4, no. 2, pp. 235–248, 2018.

[7] Z. Zhang, X. Shi, B. Wang, and H. Li, "Stability of NATM tunnel faces in soft surrounding rocks," *Computers and Geotechnics*, vol. 96, pp. 90–102, 2018.

[8] C. L. Zhang, C. P. Zhang, and J. Xu, "Comparison test of rock point load strength and uniaxial compressive strength," *Chinese Journal of Underground Space and Engineering*, vol. 11, pp. 447–451, 2015.

[9] M. C He, C. Li, W. L. Gong, J. Wang, and Z. Tao, "Support principles of NPR bolts/cables and control techniques of large deformation," *Chinese Journal of Rock Mechanics and Engineering*, vol. 35, no. 8, pp. 1513–1529, 2016.

[10] Z. G. Tao, F. Zhao, H. J. Wang, H. Zhang, and Y. Peng, "Innovative constant resistance large deformation bolt for rock support in high stressed rock mass," *Arabian Journal of Geosciences*, vol. 10, no. 15, 2017.

[11] M. He, W. Gong, J. Wang et al., "Development of a novel energy-absorbing bolt with extraordinarily large elongation and constant resistance," *International Journal of Rock Mechanics and Mining Sciences*, vol. 67, pp. 29–42, 2014.

[12] M. He, G. Zhu, and Z. Guo, "Longwall mining "cutting cantilever beam theory" and 110 mining method in China—the third mining science innovation," *Journal of Rock Mechanics and Geotechnical Engineering*, vol. 7, no. 5, pp. 483–492, 2015.

[13] Z. Tao, C. Zhu, X. Zheng et al., "Failure mechanisms of soft rock roadways in steeply inclined layered rock formations," *Geomatics, Natural Hazards and Risk*, vol. 9, no. 1, pp. 1186–1206, 2018.

[14] G. Zhou, P. Wang, C. Zou et al., "Asymmetric supporting research of god-side entry driving in complex tectonic stress mining area," *Journal of Mining & Safety Engineering*, vol. 31, no. 6, pp. 901–906, 2014.

[15] S. Dong, X. Yi, and W. Feng, "Quantitative evaluation and classification method of the cataclastic texture rock mass based on the structural plane network simulation," *Rock Mechanics and Rock Engineering*, vol. 52, no. 6, pp. 1767–1780, 2019.

[16] Y. F. Wang, X. S. Tang, Y. R. Zheng et al., "Numerical analysis of influence of rock mass joints on stability of tunneling," *Chinese Journal of Geotechnical Engineering*, vol. 35, pp. 207–211, 2015.

[17] X. Sun, G. Li, C. Zhao et al., "Investigation of deep mine shaft stability in alternating hard and soft rock strata using three-dimensional numerical modeling," *Processes*, vol. 7, no. 1, 2019.

[18] P. H. S. W. Kulatilake and B. B. Panda, "Effect of block size and joint geometry on jointed rock hydraulics and REV," *Journal of Engineering Mechanics*, vol. 126, no. 8, pp. 850–858, 2000.

[19] E. Hoek and M. S. Diederichs, "Empirical estimation of rock mass modulus," *International Journal of Rock Mechanics and Mining Sciences*, vol. 43, no. 2, pp. 203–215, 2006.

[20] E. Hoek, C. Carranza-Torres, and B. Curkum, "Hoek-Brown failure criterion—2002 edition," in *Proceedings of the Fifth North American Rock Mechanics Symposium*, vol. 1, pp. 267–273, Toronto, ON, Canada, July 2002.

[21] Itasca Consulting Group, Inc., *3DEC User Manual*, Itasca Consulting Group, Inc., Minneapolis, MN, USA, 2018.

[22] J. Wang, J. Ning, L. Jiang, J. Q. Jiang, and T. Bu, "Structural characteristics of strata overlying of a fully mechanized longwall face: a case study," *Journal of the Southern African Institute of Mining and Metallurgy*, vol. 118, no. 11, pp. 1195–1204, 2018.